RAPID COMMUNICATIONS

PHYSICAL REVIEW B VOLUME 42, NUMBER 3 15 JULY 1990-II

Rapid Communications

Rapid Communications are intended for the accelerated publication of important new results and are therefore given priority treatment both in the editorial office and in production. A Rapid Communication in **Physical Review B** *should be no longer than 4 printed pages and must be accompanied by an abstract. Page proofs are sent to authors.*

Local symmetry breaking in stage-1 alkali-metal–graphite intercalation compounds studied by scanning tunneling microscopy

D. Anselmetti, V. Geiser, G. Overney, R. Wiesendanger, and H.-J. Güntherodt
Department of Physics, University of Basel, Klingelbergstrasse 82, CH-4056 Basel, Switzerland
(Received 13 April 1990)

Scanning tunneling microscopy has been used to study surfaces of stage-1 Cs and Rb graphite intercalation compounds on the atomic scale. We have found a (2×2) superlattice as well as a one-dimensional ordering of the alkali-metal atoms corresponding to nonhexagonal $(\sqrt{3}\times4)$ and $(\sqrt{3}\times\sqrt{13})$ superlattice structures. Three rotational domains of the one-dimensional phase have been observed, inclined at 120° to each other, with sizes ranging from 10 nm to typically 60 nm. The origin of the superlattices and a transition process, based on a surface depletion of the alkali metal, are discussed.

The bulk in-plane ordering of the intercalated layers in graphite intercalation compounds[1] (GIC's) has been studied for a long time with x-ray and electron diffraction. Whereas the bulk in-plane structure of stage-1 alkali-metal GIC's has well been established, the situation in high-stage compounds is far less clear. Disordered alkali-metal layers,[2] with triangular short-range order, were detected at 300 K. A recent theoretical work[3] gives evidence of floating domains consisting of coexisting fluid and solid "phases" in unsaturated GIC's. The coexistence of several different superlattices in the bulk of high-stage Cs GIC's was first suggested on the basis of x-ray diffraction data and later confirmed by scanning transmission electron microscopy at 100 K.[4] Electron-diffraction patterns from individual structural islands identified (2×2), $(\sqrt{3}\times2)$, and $(\sqrt{3}\times\sqrt{13})$ in-plane superlattices, the latter two being nonhexagonal in-plane superlattice phases with a symmetry different from that of the graphite host lattice. The same authors analyzed the starlike electron-diffraction pattern of a stage-2 Rb GIC (which they refer to as C_VX) $(170 < T < 620$ K) (Ref. 5) to be a superposition of three nonhexagonal $(\sqrt{3}\times\sqrt{7})$, $(\sqrt{3}\times3)$, and $(\sqrt{3}\times4)$ in-plane structures. To our knowledge, the tendency of the alkali-metal atoms to form chainlike structures has not yet been theoretically treated although it is a very interesting phenomenon in quasi-two-dimensional physics.

Very recently, the in-plane ordering of the alkali-metal atoms could also be studied at the surface of alkali-metal GIC's on the atomic scale by using scanning tunneling microscopy[6] (STM) in an inert-gas environment.[7–10] On the surface of *in situ* cleaved stage-1 Li GIC's, commensurate superlattices [$(\sqrt{3}\times\sqrt{3})$ and (2×2)] as well as an incommensurate superlattice have been observed,[7,8] whereas on *in situ* cleaved C_8M (M = K, Rb, Cs) surfaces a (2×2) superlattice, which is also present in the bulk of C_8M compounds, has been found.[9,10] In this work, we report real-space observation of nonhexagonal, one-dimensional (1D) superstructures on *in situ* cleaved surfaces of well-staged C_8M compounds (M = Rb, Cs). This corresponds to $(\sqrt{3}\times4)$ and $(\sqrt{3}\times\sqrt{13})$ superlattices of the alkali-metal atoms with rectangular and centered rectangular unit cell and twofold symmetry. The one-dimensional ordering is observed in domains about 10 nm to typically 50 nm across. Macroscopically, the threefold symmetry of the underlying graphite host lattice is retained by the occurrence of three rotational domains inclined at 120° to each other. Extremely sharp domain boundaries (~0.5 nm) have been observed, indicating a very short-range driving force for the quasi-one-dimensional ordering of the alkali-metal atoms. We believe that the origin of the observed hexagonal (2×2) (Refs. 9 and 10) and the one-dimensional $(\sqrt{3}\times4)$ and $(\sqrt{3}\times\sqrt{13})$ superlattices is different, and give an explanation for a possible transition process at the surface, similar to the bulk transition process, which was attributed to a depletion of the alkali metal.[4]

The GIC samples were prepared by the standard two zone gas-phase reaction from highly oriented pyrolytic graphite (HOPG). They were characterized to be single-phase stage-1 by $(00l)$ x-ray diffraction. The scanning tunneling microscope used in this study is a commercial device,[11] which has been adapted to a stainless-steel glove box. A gas purification system lowered the O_2, N_2, and H_2O impurities in the Ar atmosphere (1 bar) beyond the detection limit of 1 ppm. The GIC samples were transferred into the Ar atmosphere without exposure to air, mechanically fixed on the sample holder stage and cleaved

prior to each measurement. We used mechanically prepared Pt-Ir tips for the STM experiments. The experimental parameters were set to 1–4 nA for the tunneling current I_t and to $\pm$(20–400) mV for the sample bias voltage U_s. All STM images were taken in the constant current mode of operation, which means that the tip followed traces of constant density of states near the Fermi energy E_F.

In Figs. 1 and 2 we present typical STM images of C_8M materials on the atomic scale. Figure 1 is a (5×6)-nm^2 image and shows the (2×2) superlattice on C_8Rb, whereas in Fig. 2 the one-dimensional $(\sqrt{3}\times4)$ superlattice on C_8Cs can be seen. The simultaneously imaged graphite lattice on both images allows an accurate determination of the superlattice orientation. In Fig. 2 the distance between the rows is exactly 4 times the graphite lattice constant of $a_0=0.246$ nm. Although a modulation along the one-dimensional structure is not detectable, we assume a $\sqrt{3}a_0$ distance between the alkali-metal atoms from the $\langle 110\rangle$ orientation of the superstructure. The observed corrugation is 0.15 ± 0.05 nm for the (2×2) superlattice, 0.05 ± 0.03 nm for the $(\sqrt{3}\times4)$ superstructure, and 0.1 ± 0.03 nm for the graphite host lattice. The bias voltage, which was set to $\pm$(20–400) mV did not influence the observed structures. The (2×2) superlattice appears always directly after cleaving the GIC sample and turned into the one-dimensional superlattice after a typical time of 20–30 min. We observed this transition many times directly on the atomic scale, where the transition took place within a few scan lines (<0.2 s) during scanning. A tip induced transition is unlikely because both superlattices could be imaged normally several hundred times without changing. In contrast to the (2×2) superlattice, where domain boundaries have not been found, we imaged several domain boundaries of the one-dimensional structures. Figure 3 is a 32×32-nm^2 image of a Rb GIC sample and shows such a domain boundary near a monatomic step of 0.35 nm in height. This agrees well with the graphite c-axis lattice constant. In contrast to the lower terrace, where the one-dimensional superlattice with the domain boundary was imaged, only the regular hexagonal graphite lattice was observed on the upper terrace. The 6.5×6.0-nm^2 STM image (Fig. 4) is a closer look at the domain boundary and corresponds to the marked section in Fig. 3. Here another superlattice can be seen. This domain consists of one-dimensional chains, which are separated alternatingly by 4 and 3.5 times a_0, the lattice constant of graphite. We interpret this as an alternating $(\sqrt{3}\times4)$ and $(\sqrt{3}\times\sqrt{13})$ arrangement of the alkali-metal atoms. A high-resolution image of domain boundaries on Rb GIC is shown in Fig. 5, where three different domains inclined at 120° to each other are visible. The boundary zone has a width of ~0.5 nm. No defect in the HOPG

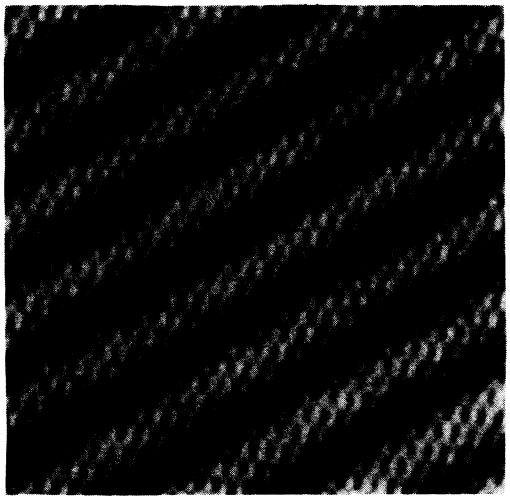

FIG. 2. On this 7.5×6.5-nm^2 image ($U_s=-160$ mV, $I_t=1.5$ nA) of CsC_8 the chainlike $(\sqrt{3}\times4)$ superstructure and the underlying HOPG lattice can be seen.

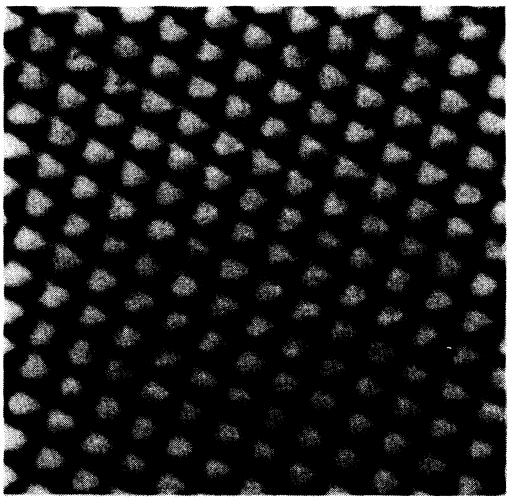

FIG. 1. STM image ($U_s=50$ mV, $I_t=3.4$ nA) of RbC_8, which shows the (2×2) superlattice with the underlying HOPG lattice on a 5.0×6.0-nm^2 area.

FIG. 3. STM image of RbC_8 (32×32 nm^2, $U_s=42$ mV, $I_t=2.6$ nA), which shows a domain boundary of the one-dimensional superlattices near a surface step.

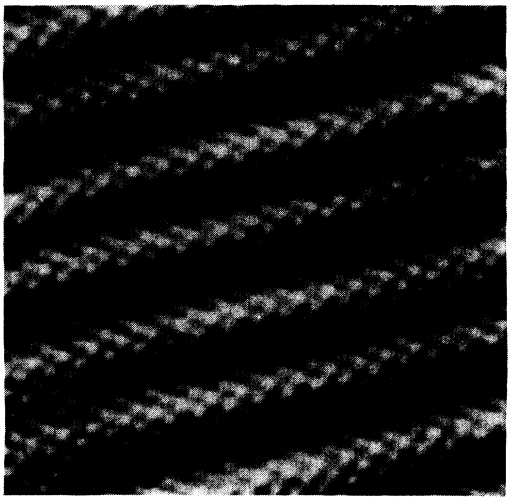

FIG. 4. This image (6.5×6.0 nm^2, $U_s=42$ mV, $I_t=2.6$ nA) corresponds to the marked section in Fig. 3. The alternating distances of $3.5a_0$ and $4a_0$ between the one-dimensional superstructures are clearly visible.

lattice can be seen, which might induce this domain formation.

The stoichiometric composition of the observed $(\sqrt{3}\times4)$ superlattice is $C_{16}M$. Assuming an initial (2×2) superlattice for C_8M GIC's, this would correspond to a surface depletion, most likely due to a desorption process of the alkali metal into the argon atmosphere. A diffusion process into the bulk is unlikely, because of the saturated low-lying graphite galleries in stage-1 GIC's. A severe influence of reaction products (e.g., recombinations of atmospheric impurities with alkali-metal atoms) to this surface depletion also seems to be unlikely, because of the abrupt transition on a large scale as well as the permanent ideal experimental conditions, which should be severely disturbed on the atomic scale by a contamination layer. The nonobservation of this one-dimensional superlattice structure on C_6Li and C_8K also excludes an impurity driven transition or strain effects due to the sample mounting or sample cleaving procedure. Furthermore, a more complex arrangement of the alkali-metal atoms for explaining the one-dimensional superstructures with an unchanged C_8M composition is unlikely because of the regularity of the observed superstructures as well as the observation of a depleted graphitic surface structure after 2–3 d.

Two experimental results differ for the observed superlattices. First, the corrugation amplitude of the (2×2) superlattice is about 2–3 times larger than for the $(\sqrt{3}\times4)$ superlattice. Second, we observe a different spatial resolution of ~0.25 nm for the hexagonal and ~0.5 nm for the one-dimensional superlattice by using the same STM tip.

Besides the understanding of the formation of different superlattices, the question, concerning the location of the alkali-metal atoms, plays an important role. We have two possible interpretations for the observed structures. The large corrugation for the (2×2) superlattice suggests an enhanced topographic effect or a special electronic state near E_F. The latter case might be supported by angle-resolved photoemission spectroscopy (ARPES) experiments on C_8Cs,[12] giving evidence for a low-dispersion band near E_F, which might have its origin in a surface driven charge-density wave (CDW). This was also suggested by Kelty and Lieber.[10] In case of a surface depletion of the intercalated material, one can expect an energetically favored one-dimensional reorientation of the alkali-metal atoms. The loss in spatial resolution by undergoing this transition is difficult to understand with a simple rearrangement of the alkali-metal atoms at the surface, but might be understood with a simultaneous collapse of the assumed surface CDW.

One can also think of a drastic change in the electronic properties from electronically isolated atoms to metallically bonded alkali-metal atoms (1D alkali metal), caused by an atom separation of $\sqrt{3}a_0$ ($=0.429$ nm), which is smaller than the nearest-neighbor distance in the 3D metal. For this case no theoretical work is known to the authors. In contrast, the deformation of the topmost graphite layer due to an intercalated alkali-metal atom in the first graphite gallery has recently been treated theoretically.[13] Applied to the observed one-dimensional superlattice structures, this would allow a first estimate for the healing

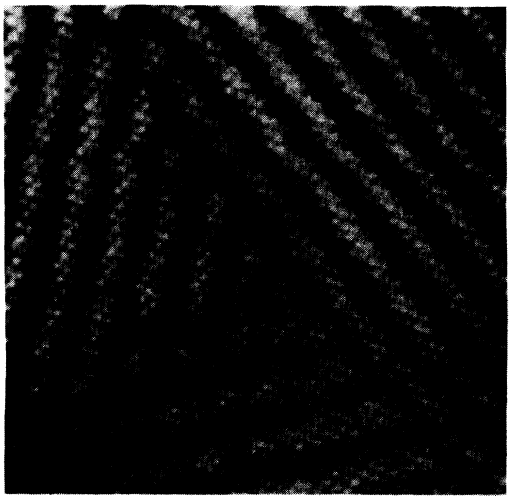

FIG. 5. Three rotational $(\sqrt{3}\times4)$ domains are shown in this 10.0×9.0-nm^2 image of RbC_8 ($U_s=20$ mV, $I_t=2.0$ nA).

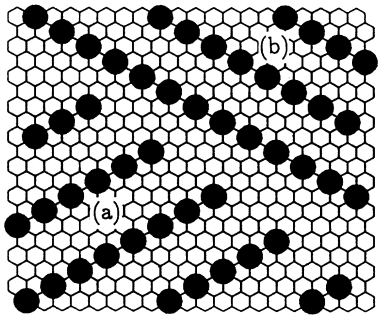

FIG. 6. (a) The $(\sqrt{3}\times4)$ and (b) the $(\sqrt{3}\times\sqrt{13})$ superlattice are schematically shown with the underlying HOPG honeycomb lattice.

length λ_i, which corresponds to the distance at which the layer distortion decreases to its half maximum value. The measured healing length ($\sim$0.25 nm) and the height variation ($\sim$0.05 nm) of these superstructures are in excellent agreement with this theoretical prediction and would therefore be the first local real-space evidence for a decrease of the flexural rigidity of a single graphite layer upon intercalation, as it was measured in neutron-diffraction experiments.[14] As mentioned above, an interesting point concerns the supposed in-row distance of $\sqrt{3}a_0$ ($=$0.426 nm) of the Rb and the Cs atoms in the $(\sqrt{3}\times 4)$ and $(\sqrt{3}\times\sqrt{13})$ (Fig. 6) structures, which is smaller than the regular bulk separation in the hexagonal (2×2) superlattice. If one compares this in-row distance with the width of the one-dimensional superstructures of $\sim$0.5 nm, it is obvious that a STM resolution of the alkali-metal sites along the superlattice structure is very difficult to achieve.

In summary, we have investigated stage-1 C_8M GIC (M=Rb, Cs) on the atomic scale by STM. For the first time we have observed one-dimensional superlattices $[(\sqrt{3}\times 4)$ and $(\sqrt{3}\times\sqrt{13})]$ with domain sizes ranging from 10 to 60 nm besides the hexagonal (2×2) superlattice on these surfaces. We have evidence that the surface of stage-1 GIC's in an inert-gas atmosphere gets depleted and can be compared with the bulk of high-stage GIC's.[4] The origin of the observed superlattice structures is discussed and compared with ARPES experiments and a recent theoretical work.

We would like to thank Dr. A. W. Moore for providing HOPG. Financial support from the Swiss National Science Foundation is gratefully acknowledged.

[1]M. S. Dresselhaus and G. Dresselhaus, Adv. Phys. **30**, 139 (1981).

[2]R. Clarke, N. Caswell, S. A. Solin, and P. M. Horn, Phys. Rev. Lett. **43**, 2018 (1979).

[3]J. D. Fan, G. Reiter, and S. C. Moss, Phys. Rev. Lett. **64**, 188 (1990).

[4]D. M. Hwang, N. W. Parker, M. Utlaut, and A. V. Crewe, Phys. Rev. B **27**, 1458 (1983).

[5]N. Kambe, G. Dresselhaus, and M. S. Dresselhaus, Phys. Rev. B **21**, 3491 (1980).

[6]G. Binnig, H. Rohrer, Ch. Gerber, and E. Weibel, Phys. Rev. Lett. **49**, 57 (1982).

[7]D. Anselmetti, R. Wiesendanger, and H.-J. Güntherodt, Phys. Rev. B **39**, 11 135 (1989).

[8]D. Anselmetti, R. Wiesendanger, V. Geiser, H. R. Hidber, and H.-J. Güntherodt, J. Mirosc. **152**, 509 (1988).

[9]S. P. Kelty and C. M. Lieber, J. Phys. Chem. **93**, 5983 (1989).

[10]S. P. Kelty and C. M. Lieber, Phys. Rev. B **40**, 5856 (1989).

[11]Nanoscope II, Digital Instruments Inc., Santa Barbara, CA.

[12]M. Laguës, J. E. Fischer, D. Marchand, and C. Fretigny, Solid State Commun. **67**, 1011 (1988).

[13]D. Tománek, G. Overney, H. Miyazaki, S. D. Mahanti, and H.-J. Güntherodt, Phys. Rev. Lett. **63**, 876 (1989).

[14]H. Zabel, in *Graphite Intercalation Compounds,* edited by H. Zabel and S. A. Solin, Topics in Current Physics (Springer-Verlag, New York, 1989).

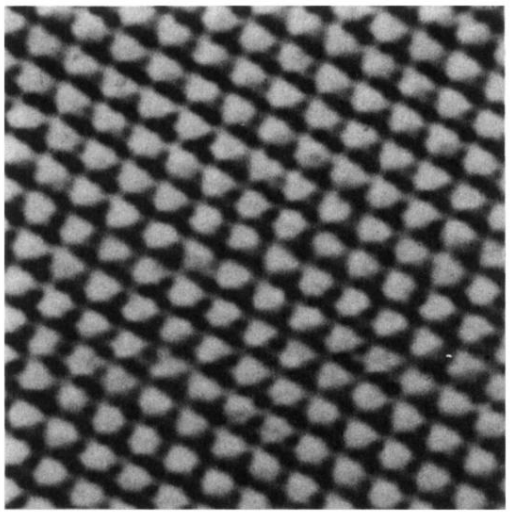

FIG. 1. STM image ($U_s = -50$ mV, $I_t = 3.4$ nA) of RbC_8, which shows the (2×2) superlattice with the underlying HOPG lattice on a 5.0×6.0-nm^2 area.

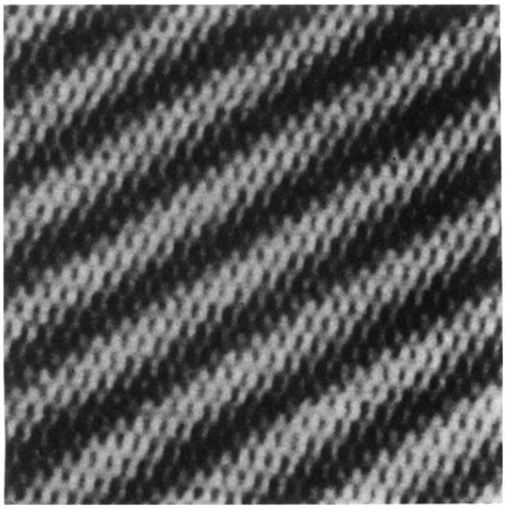

FIG. 2. On this 7.5×6.5-nm^2 image ($U_s=-160$ mV, $I_t=1.5$ nA) of CsC_8 the chainlike $(\sqrt{3}\times4)$ superstructure and the underlying HOPG lattice can be seen.

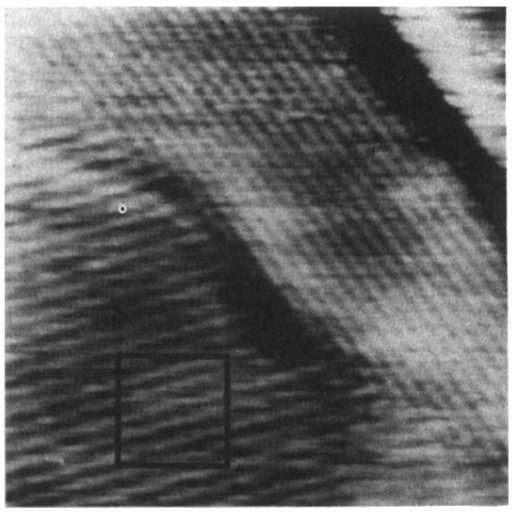

FIG. 3. STM image of RbC_8 (32×32 nm^2, $U_s=42$ mV, $I_t=2.6$ nA), which shows a domain boundary of the one-dimensional superlattices near a surface step.

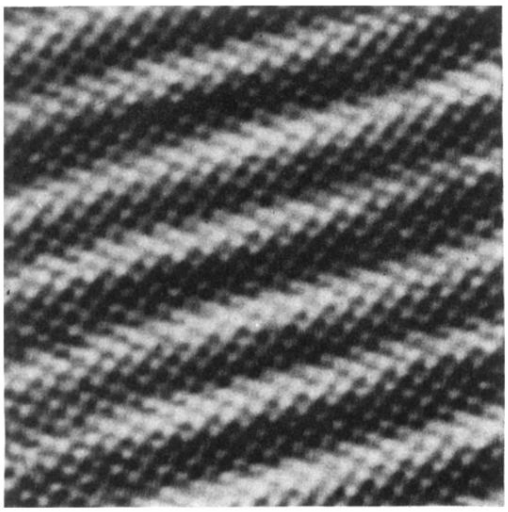

FIG. 4. This image (6.5×6.0 nm^2, $U_s = 42$ mV, $I_t = 2.6$ nA) corresponds to the marked section in Fig. 3. The alternating distances of $3.5a_0$ and $4a_0$ between the one-dimensional superstructures are clearly visible.

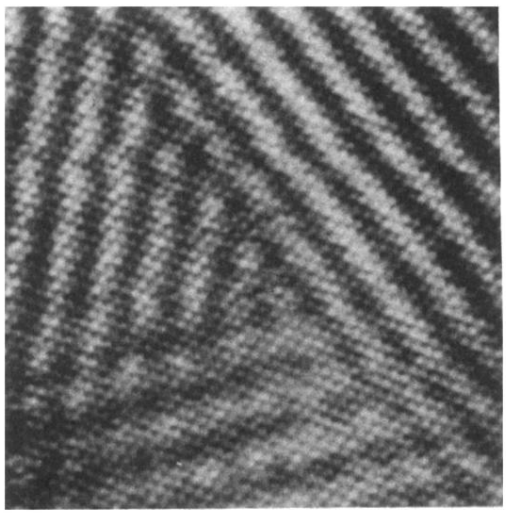

FIG. 5. Three rotational $(\sqrt{3}\times 4)$ domains are shown in this $10.0\times 9.0\text{-nm}^2$ image of RbC_8 ($U_s = 20$ mV, $I_t = 2.0$ nA).